Thermal variation at different penetration angle for orthopaedic surgical bone drilling

M.S.Noorazizi[1,2*], R.Izamshah[2], M.Hadzley[2], M.S Kassim[2]

[1)] Faculty of Manufacturing Engineering, Universiti Teknikal Malaysia Melaka, Hang Tuah Jaya, 76100 Durian Tunggal, Melaka, Malaysia

[2)] Advanced Manufacturing Centre, Faculty of Manufacturing Engineering, Universiti Teknikal Malaysia Melaka, Hang Tuah Jaya, 76100 Durian Tunggal, Melaka, Malaysia

[*]Corresponding e-mail: engr.nms801@gmail.com.

Keywords: Thermal necrosis; penetration angle; surgical drill

ABSTRACT – Thermal necrosis developed on soft tissues around the hole during a surgical procedure orthopedic bone drilling. It happens due to the friction between the drill and the bone surface which leads to a local increase in temperature. The magnitudes of the friction energy are greatly dependant on the drill geometry design. Recognizing the importance of the phenomenon, this paper aims to investigate the effects of drill geometry on temperatures rises during bone drilling procedure. A total of 17 drills was made at different geometry namely point angle, helix angle and web thickness, penetrated at angles of 0^0, 15^0, and 30^0 to mimic a manual control penetration by a surgeon. It was found that the most significant parameter that affect the temperature rises is the penetration angle followed by the point angle. In addition, an interaction between helix angle and web thickness also control the drilling temperature.

1. INTRODUCTION

One of the principal methods for repairing and reconstruction of a bone fracture are achieved by drilling the bone and fixing the separate parts together using screws, wires and plates. Many problems are encountered with the bone drilling process such as holes accuracy, drill wander and excessive heat generation which were directly related with the drilling parameter [1,7]. Many different drill-bit designs and geometries have been suggested over the years each with its own promising results [2,3]. However, most of the studies neglected the effects of penetration angle on the drilling performances. Generally, in normal orthopedic surgery, bone drilling is performed using hand drills and the penetration angles is greatly dependent on the surgeon's manual skill and are normally deviated from the normal axis. Thermal necrosis is a common phenomenon during the bone drilling procedure due to the sensitivity of the soft tissue surrounding the bone [3]. Ideally, the generated drilling temperature must be below 47°C in order to avoid thermal necrosis [4,6,7]. The magnitudes of the drilling temperature are greatly dependant on the drill geometry design and should be methodically analyse to control the temperature rise.

2. EXPERIMENTAL WORK

In this experiment, AISI 420B stainless steel medical grade rod with diameter 4.3 mm were ground to form the drill bits as shown in figure 1 with varying angles namely point angle, helix angle and web thickness as depicted in Table 1. Stainless steel drill bit exhibits good corrosion resistance and can minimize the tool wear effect. Totals of 51 holes were drilled with 3 holes replication for each run. To eliminate the apparatus wear impact on the result, the apparatus were cleaned with a brush and wet tissue before each drilling process.

Table 1 Drill geometrical angles design level

	Name	Unit	Low	High
A	Web Thickness	%	14	32
B	Point Angle	°	90	140
C	Helix Angle	°	16	38
D	Penetration Angle	°	0	30

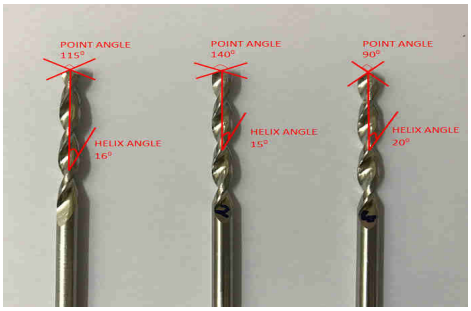

Figure 1 Three (3) sample design of 17 drill bit

Bovine cortical femur bone was chosen as the work material due to its closeness properties and characteristics with human bone [5-7]. Fresh cortical (compact bone) samples are cuts and mills from bovine femur with a uniform thickness of 4 mm as shown in Figure 2. The drilling tests were performed using a DMU60 monoBLOCK DECKEL MAHO CNC 5-Axis Machine. The drilling speed of 1000 rpm and 100 mm/min feed rate were employed to represent the actual manual surgical hand drills speed and surgeon penetration feed. The drilling temperatures were measured using portable thermal infrared camera Thermal Cam FlirOne. The camera was positioned so as not to interfere with the drilling process and simultaneously take full advantage of the environment and light available as shown in figure 3.

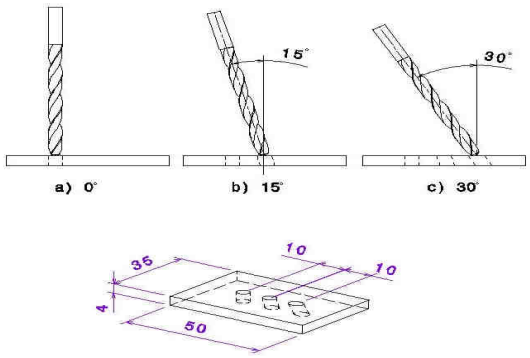

Figure 2 Bone work-pieces with its drilling cutting angle (0^0, 15^0, and 30^0).

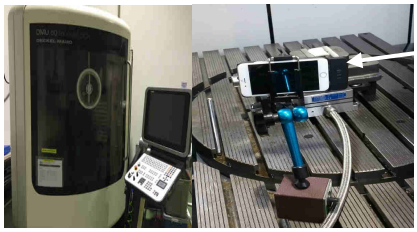

Figure 3 Experimental layout

3. RESULTS AND DISCUSSION

The effects of drill geometries such as point angle, web thickness and helix angle has deep effect on the temperature rise. From the conducted experimental tests, it is evidently shows the variation of drilling temperature on different drills design as well with the variation on penetration angle.

Table 2 Experimental temperature result

RUN	F1	F2	F3	F4	R1	RUN	F1	F2	F3	F4	R1
	A	B	C	D	Temp.		A	B	C	D	Temp.
1	23	115	27	0	31.2	**27**	32	90	27	15	58.4
2	14	140	27	0	41.6	**28**	23	115	27	15	31.3
3	14	90	27	0	48	**29**	23	90	38	15	34.5
4	23	115	27	0	35	**30**	32	115	38	15	30.1
5	14	115	16	0	33.1	**31**	23	90	16	15	32.4
6	23	115	27	0	31	**32**	23	115	27	15	29.5
7	14	115	38	0	31	**33**	23	140	16	15	59
8	23	140	38	0	30.8	**34**	32	115	16	15	28.8
9	32	140	27	0	49	**35**	23	115	27	30	39.1
10	32	90	27	0	58	**36**	14	140	27	30	35
11	23	115	27	0	29.1	**37**	14	90	27	30	30.6
12	23	90	38	0	28	**38**	23	115	27	30	43.9
13	32	115	38	0	28.8	**39**	14	115	16	30	45.1
14	23	90	16	0	35	**40**	23	115	27	30	31.7
15	23	115	27	0	28.8	**41**	14	115	38	30	35.6
16	23	140	16	0	28	**42**	23	140	38	30	33.5
17	32	115	16	0	29	**43**	32	140	27	30	35.8
18	23	115	27	15	29.3	**44**	32	90	27	30	62.2
19	14	140	27	15	61.2	**45**	23	115	27	30	32.4
20	14	90	27	15	29.5	**46**	23	90	38	30	37.6
21	23	115	27	15	40.4	**47**	32	115	38	30	31.2
22	14	115	16	15	40.2	**48**	23	90	16	30	48.7
23	23	115	27	15	30.9	**49**	23	115	27	30	30.5
24	14	115	38	15	36.7	**50**	23	140	16	30	58.8
25	23	140	38	15	33.2	**51**	32	115	16	30	30.1
26	32	140	27	15	50.7						

Table 2 shows the experimental results for all runs. The minimum drilling temperature obtained was 28°C from drill design no.16 at 0° penetration angle condition. While the highest recorded temperature was 62.2°C for drill design no. 44 at 30° penetration angle condition. Figures 4 show the screenshot of the minimum and maximum recorded temperatures.

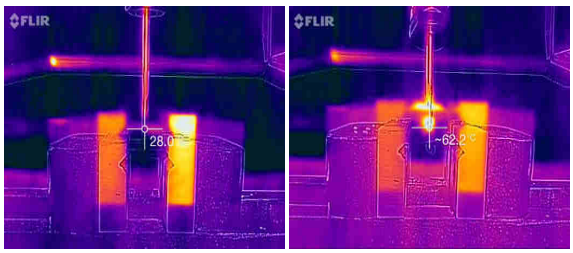

a) b)

Figure 4 Recorded temperature a) Min = 28 °C at 0^0 PA, b) Max = 62.2 °C at 30^0 PA.

4. CONCLUSIONS

A practical investigations on the effects of drilling temperature with different drill geometry parameters were studied. This study demonstrated the interaction on the effects of drill-bit design geometry parameters with temperature for different drilling angle conditions. The interaction between the design geometry parameter and the drilling angle significantly affect the temperature magnitudes. It can be stated that the temperature increases with an increasing in the drilling penetration angle and the increases of point angle whereas the web thickness and helix angle at the middle level generate the lowest temperature. To conclude, the results from the conducted experiments provide the reference values for the development of high performance surgical drill design in orthopedic bone surgeries application.

REFERENCES

[1] R Izamshah, MS Noorazizi, MS Kasim, CHC Haron. "Influence of Orthopaedic Drilling Parameters on Surface Roughness and Cutting Force of Bone Drilling Process". *Atlantis Press Publishing*. 2016.

[2] M.T. Hillery and I. Shuaib. "The drilling of bone using guide wires and twist drills". *IMC-13*, Ireland, (1996) pp. 33-42. 1996.

[3] R. K. Pandey and S. S. Panda. "Drilling of bone: A comprehensive review". Journal of Clinical Orthopaedics and Trauma. 4(1): 15-30. 2013.

[4] R. Eriksson and R. Adell. "Temperature during drilling for placement of implants using osseointegration technique". *J. Oral Maxillofac Surg*. 44: 4–7. 1986.

[5] Vashishth, D., Tanner K.E. and Bonfield W. "Contribution, development and morphology of microcracking in cortical bone during crack propagation". *Journal of Biomechanics*. 33: 1169-1174. 2000.

[6] Alam K., Khan M., Muhammad R., Qamar SZ, and Silberschmidt. "In-vitro experimental analysis and numerical study of temperature in bone drilling". *Technol. Health Care*. 23(6): 775-783. 2015.

[7] G. Augustin, T. Zigman, S. Davila, T. Udilijak, T. Staroveski, D. Brezak and S. Babic. "Cortical bone drilling and thermal osteonecrosis". *Clinical Biomechanics*. 27(4): 313-325. 2012.

Development of an integrated ANP and TRIZ for new framework of design selection for automotive at the conceptual design stage

M.T Amira Farhana*, A. Hambali, A.M. Mohd Edeerozey

Faculty of Manufacturing Engineering, Universiti Teknikal Malaysia Melaka, Hang Tuah Jaya, 76100 Durian Tunggal, Melaka, Malaysia

*Corresponding e-mail: amirafarhana.mtar@gmail.com

Keywords: ANP; TRIZ; Automotive

ABSTRACT –Finding solution in conceptual design has to deal with the multi-decision methods. This paper aimed to develop a new framework of design selection during conceptual design stage for automotive part. The framework consists of integrated methods of multi-decision methods and problem solving for contradiction issues. Thus, ANP and TRIZ is integrate to generate new integrated method for conceptual design stage.

INTRODUCTION

Design selection in automotive field required the best design tools to create the excellent part of automotive systems. Therefore, in designing concept, the conceptual stage had to deal with the design selection method based on the current product design. Conceptual design is considered as the most creative, complicated and difficult stage in the product development, which implies that designers need broad cross-disciplinary knowledge, complex technical support and sound design theory to acquire design concepts [1].

Using the integrated method of ANP and TRIZ, the framework is developed to propose a new system of design selection for automotive. Since many decision problems cannot be structured hierarchically, the Analytic Network Process (ANP) method is generate from previous method that is Analytic Hierarchy Process (AHP) which ANP has the ability to accommodate the relationship between criteria or alternatives [2]. The generalization from AHP system to ANP system is shown in Figure 1.

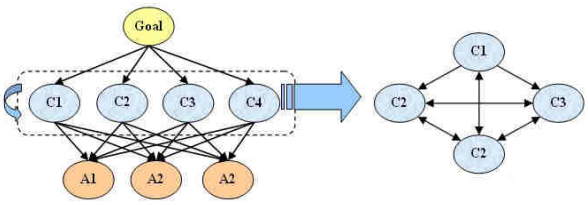

Figure 1 Generalization of hierarchy to network structure.

By solving some issues, one must utilize the best methods concept of resolving the contractions as the demanding technology race against time. TRIZ is a potential solution involving contradiction matrix comprising 40 Principles and 39 Parameters and the best inventive principle will be selected for innovative design of the product [3,4]. The TRIZ way of problem solving as shown in Figure 2.

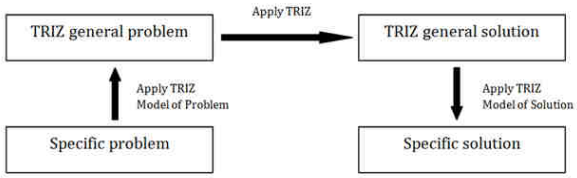

Figure 2 TRIZ Way of problem solving

METHODOLOGY

2.1 Analytic Network Process (ANP)

Analytic Network Process (ANP) consists of four (4) general steps in ANP including model construction; paired comparisons between each two clusters or nodes; super matrix calculation based on results from paired comparisons and result analysis for the assessment [5,6]. ANP method has the ability to accommodate the relationship between criteria or alternatives, where it can improve the weakness of AHP method. ANP uses a network without the need to specify levels as in a hierarchy [7]. By replacing hierarchies with networks, ANP has generally utilized in multi criteria decision making tool which is the AHP [8]. The ANP is put together with the fuzzy approach to prevent any uncertainties with its conventional in conceptual design alternative selection in a new product development environment to achieve most fulfilling needs and expectations of the customers as their opinion will always be differ with engineering specification of OEM [9,10].

2.2 Theory of Inventive Problem Solving (TRIZ)

TRIZ is a Russian acronym for "Teoriya Resheniya Izobreatatelskikh Zadatch" stands for "Theory of Inventive Problem Solving"[3]. TRIZ focused on problem understanding to the particular, relevant issue model and then generate conceptual solutions to the model [11]. TRIZ act as a methodology for the effective development of new technical system and being a set of principle to show how the technologies and system work

out [12]. The aim of TRIZ is to overcome the physical obstacle in problem solving through the generalization of the specific problem to an correspondent generic problem where it can develop a generic solution [11,13].

EXPECTED RESULT

The Integrated of ANP and TRIZ develop a new framework to select the best design in conceptual design stage. The automotive part selected is a front bumper part; fascia which the part will be analyse using the integrated framework. Using Mind Decider Pro as shown in Figure 3, each of the criteria is filled in the network structure followed by the subcriteria to generate the alternatives in terms of independence or dependence (loops) that connect a component to itself. The element has its own ranking based on the weightage which will form into supermatrix of network. The curve represent the loops of the subcriteria where the subcriteria depends on itself using network system (dependence). The calculation at the end will give out the best result. Thus, it will be use in the integrated framework to achieve the selection of design in the conceptual stage. TRIZ tools is used in the early stage of the loops to solve the issue and substitute in each feedback.

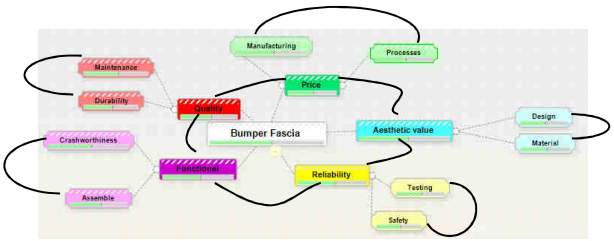

Figure 3 Network structure, dependence and feedback

ACKNOWLEDGEMENT

The authors are grateful to Universiti Teknikal Malaysia Melaka and Ministry of Higher Education, Malaysia for financially supporting this project under research grant numbered FRGS/2/2013/TK04/FKP/02/F00179.

REFERENCES

[1] Yu KM, Lau CT, Tong KL, Wong WK. Integrated conceptual design with TRIZ. TRIZ J 2008. <https://triz-journal.com/integrated-conceptual-design-with-triz> (cited 12.04.13).

[2] Saaty, T. L. (2004). Decision making — the Analytic Hierarchy and Network Processes (AHP/ANP). Journal of Systems Science and Systems Engineering, 13(1), 1-35. doi:10.1007/s11518-006-0151-5

[3] San, Y. T., Jin, Y. T., & Li, S. C. (2009). TRIZ: Systematic innovation in manufacturing. Petaling Jaya, Malaysia: Firstfruits Sdn. Bhd.

[4] Vinodh, S., Kamala, V., & Jayakrishna, K. (2014). Integration of ECQFD, TRIZ, and AHP for innovative and sustainable product development. Applied Mathematical Modelling, 38(11-12), 2758-2770. doi:10.1016/j.apm.2013.10.057

[5] Saaty, Thomas L. (1996), Decision Making with Dependence and Feedback: The Analytic Network Process, RWS Publications, 4922 Ellsworth Avenue, Pittsburgh, PA. 15213.

[6] Saaty, Thomas L. (1997), the Analytic Network Process, RWS Publications, 4922 Ellsworth Avenue, Pittsburgh, PA 15213.

[7] Saaty, T. L. (1999, August). Fundamentals of The Analytic Network Process. International Symposium on the Analytic Hierarchy Process (ISAHP), 1-14.

[8] Büyüközkan, G., & Berkol, Ç. (2011). Designing a sustainable supply chain using an integrated analytic network process and goal programming approach in quality function deployment. Expert Systems with Applications. doi:10.1016/j.eswa.2011.04.171.

[9] Chen, H.H., Kang, H.Y., Xing, X., Lee, A.H.I. and Tong, Y. (2008), "Developing new products with knowledge management methods and process development management in a network", Computers in Industry, Vol. 59 Nos 2/3, pp. 242-253.

[10] K, J., K.e.k, V., & Vinodh, S. (2015). ANP based sustainable concept selection. Jnl of Modelling in Management Journal of Modelling in Management, 10(1), 118-136. doi:10.1108/jm2-12-2012-0042.

[11] Gironimo, G. D., Carfora, D., Esposito, G., Labate, C., Mozzillo, R., Renno, F., . . . Siuko, M. (2013). Improving concept design of divertor support system for FAST tokamak using TRIZ theory and AHP approach. Fusion Engineering and Design, 88(11), 3014-3020. doi:10.1016/j.fusengdes.2013.07.005.

[12] Fey, V., Rivin, E.I., 2005. Innovation on Demand: New product development using TRIZ. Cambridge University Press, Cambridge, UK.

[13] J. Terninko, A. Zusman, B.Zlotin, Systematic Innovation – An Introduction to TRIZ (Theory of Inventive Problem Solving), St. Lucie Press, USA 1998.

Proceedings of Innovative Research and Industrial Dialogue'16, pp. 125-126 (May 2017)

The evaluation of Mandarin MOOC: A case study of effectiveness

S. F. Ahmad Fesol*, S. Salam

Faculty of Information and Communication Technology, Universiti Teknikal Malaysia Melaka, Hang Tuah Jaya, 76100 Durian Tunggal, Melaka, Malaysia

*Corresponding e-mail: feyrs88@gmail.com

Keywords: Open online course; student effectiveness; MOOC learning design

ABSTRACT – Measuring the learning outcome is a crucial part in evaluating the effectiveness of the teaching and learning process. The students' feedback provided will allow the educators to improve the teaching strategy in order to engage the students more via online learning. Thus, the objective of this study is to evaluate the effectiveness of Mandarin Massive Open Online Course (MOOC) based on students' evaluation. This study used descriptive based analysis in order to analyze the data gathered. An online survey approach was employed. It consists of 24 items which were categorized into four dimensions namely as learning design, content design, learning attitude and enhancement in teaching & learning. The findings revealed that as much as 115 out of 123 respondents (94%) do agree that learning Mandarin through MOOC is effective, able to help them to improved their understanding and help them meeting their learning goals.

1. INTRODUCTION

In every curriculum course design, evaluation process is one of the most important and critical step [1-2]. Evaluation as per defined by Mary Thorpe [3] is a collection, analysis and interpretation of information about any aspect of a programme of education or training, as part of a recognized process of judging its effectiveness, its efficiency and any other outcomes it may have [3]. Usually, this step is placed as the final stage and trying to figure out either the course structure is effective and efficient enough to support the teaching and learning process or not. Moreover, feedback from the assessment and evaluation can be used by educators to improved and refine the current course structure in order to engage the students more with the learning as well as helping the students to meet the learning objectives. There are a lot of MOOC models and frameworks which can be used to evaluate MOOC effectiveness as per proposed by [4-6]. However, in this study we adopted and improvised a framework as per suggested by [7] which consist of four dimensions. The same framework also has been used by other researches in finding the MOOC effectiveness of MOOC pilot testing in Malaysia [7].

2. METHODOLOGY

A quantitative based method was chosen as the blue print in this study. Online based questionnaire was used as the main data collection method that students filled in at the end of the course. The questionnaire consists of 24 items that formed four dimensions of MOOC effectiveness model. The dimensions were learning design, content design, learning attitude, and enhancement in teaching & learning with each items scored from 1 (strongly disagree); 2 (somewhat disagree); 3 (somewhat agree); 4 (strongly agree); to 5 (completely agree) options. There is a total of 123 valid respondents (n=123) who possess engineering background education. Among them, 45.5% are female and remaining 54.5% are male respondents. Figure 1 illustrates the overall picture of learning design adopted in this Mandarin MOOC.

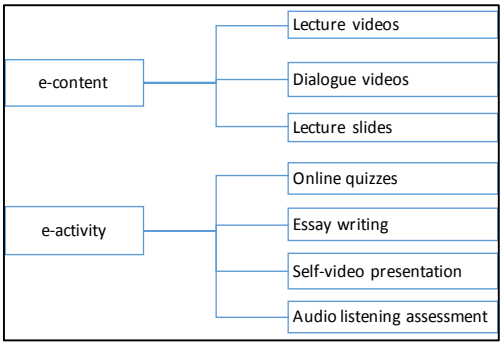

Figure 1 Mandarin MOOC learning design.

In order to identify the reliability for each of the construct used, Cronbach-Alpha test was implemented. The results revealed that all the constructs used reflected as acceptable (above .70) and preferable (above .80) [8]. Table 1 presents the Cronbach-Alpha value and number of items for each of the construct.

Table 1 Cronbach-alpha value for each construct.

Construct	Reliability	Item
Learning design (LD)	0.931	4
Content design (CD)	0.912	9
Learning attitude (LA)	0.919	5
Enhancement in T&L (E)	0.939	6

3. RESULT AND DISCUSSION

The data gathered were analyzed using descriptive analysis. From the learning design dimension analysis as illustrated in Table 2, data shows that majority of the respondents decided between somewhat agree and strongly agree that the course is well design (LD1);

learning through MOOC meets their learning needs (LD2); the sequence of learning activities help my understanding of the subject matter (LD3); and the learning schedule prepared by instructors suits their learning pace (LD4). Regarding the content design dimensions, the overall data reflects that majority of the respondents indicated between somewhat agree and strongly agree that the course materials covers the essential aspects of the course (CD1); the course materials is well organized (CD2); the course materials are clear (CD3); the course activities and course materials able to enhance their understanding of the topic covered (CD4 & CD5); the course materials and course activities provided meet their learning needs (CD6 & CD7); and the course materials (e-content) and course activities (e-activities) are useful for their learning (CD8 & CD9).

In terms of learning attitude dimensions, the analysis uncovers that majority of the respondents do agree that they able to follow the course at their own pace (LA1); they able to accomplish the course activities on their own (LA2); learning using MOOC allows personalization (students can interact one-to-one with the instructor) (LA3); and also the respondents do engage more with lecture video and dialogue video to understand better (LA4& LA5). Further analyzing from the enhancement in T&L dimensions, data clarifies that majority of the respondents once again do somewhat agree and strongly agree that MOOC enhances their learning experience (E1); learning via MOOC is enjoyable (E2); they learn more effective using MOOC (E3); they satisfied in learning using Mandarin MOOC (E4); they believe the use of MOOC for learning Mandarin is feasible (E5); and learning via MOOC help them to remember, understand and apply the learning more effective (E6). Table 2 summarized the mean and standard deviation by each item.

Table 2 Distribution of mean and standard deviation by each item.

Item	Mean	SD
LD1	3.63	0.78
LD2	3.62	0.74
LD3	3.67	0.74
LD4	3.64	0.81
CD1	3.72	0.77
CD2	3.76	0.71
CD3	3.81	0.73
CD4	3.71	0.78
CD5	3.75	0.76
CD6	3.72	0.75
CD7	3.73	0.79
CD8-1	3.91	0.79
CD8-2	3.89	0.80
CD8-3	3.93	0.73
CD9-1	3.35	1.09
CD9-2	3.07	1.00
CD9-3	3.22	1.07
CD9-4	3.29	1.03
LA1	3.57	0.75
LA2	3.59	0.73
LA3	3.56	0.75
LA4	3.82	0.77
LA5	3.73	0.77
E1	3.78	0.83
E2	3.73	0.79
E3	3.75	0.81
E4	3.82	0.84
E5	3.84	0.79
E6-1	3.87	0.69
E6-2	3.89	0.71
E6-3	3.89	0.69

4. CONCLUSSION

Overall, the result of this study offers some implications in the learning environment. Firstly, the analysis summarized that as much as 94 per cent (115 respondents) agreed that learning through MOOC is effective, able to help them to improved their understanding and help them meeting their learning goals, same results as reported by [2,5-7]. In addition, from Mandarin MOOC learning design and framework as per exemplify earlier in this research, it can become a guideline to educators in preparing and creating an effective MOOC course.

5. ACKNOWLEDGEMENT

The authors would like to take this opportunity to highly appreciate the cooperation and the opportunity given by UTeM organization and UTeM Zamalah Scheme for funding this research.

REFERENCES

[1] P. McGee and A. Reis, "Blended Course Design: A Synthesis of Best Practices," *Journal of Asynchronous Learning Networks*, 16(4), 2012, pp. 7-22.

[2] S. Cooper and M. Sahami, "Reflections on Stanford's MOOCs," *Communications of the ACM*, 56(2), 2013, pp. 28-30.

[3] M. Thorpe, *Evaluating open and distance learning*, Harlow: Longman, 1993.

[4] D. Gamage, I. Perera and S. Fernando, "A Framework to analyze effectiveness of eLearning in MOOC: Learners perspective," *Ubi-Media Computing (UMEDIA), 2015 8th International Conference*, 2015, pp. 236-241.

[5] T. Daradoumis, R. Bassi, F. Xhafa and S. Caballé, "A review on massive e-learning (MOOC) design, delivery and assessment," *P2P, Parallel, Grid, Cloud and Internet Computing (3PGCIC), 2013 Eighth International Conference,* 2013, pp. 208-213.

[6] F. Brouns, J. Mota, L. Morgado, D. Jansen, S. Fano, A. Silva and A. Teixeira, "A networked learning framework for effective MOOC design: the ECO project approach.," 2014.

[7] H. A. Jalil, A. Ismail, N. Bakar and N. A. K. K. A. Nasir, "Evaluation of Malaysia Pilot MOOC (Final Report)," 2016.

[8] J. Pallant, *SPSS survival manual: A step-by-step guide to data analysis using SPSS, vol. 15*, Nova Iorque: McGraw Hill, 2007.

Proceedings of Innovative Research and Industrial Dialogue'16, pp. 127-128 (May 2017)

Interpretation of ISO 6983 and ISO 14649 for CNC adaptive controller: plug-and-play interpreter

M.A.Othman, M.Minhat*, Z.Jamaludin, N.M.Seman

Faculty of Manufacturing Engineering, Universiti Teknikal Malaysia Melaka, Hang Tuah Jaya, 76100 Durian Tunggal, Melaka, Malaysia

*Corresponding e-mail: mohdm@utem.edu.my

Keywords: STEP-NC; interpreter; function block

Abstract – Interpreter is a software module inside a CNC controller, which extract the data of NC part program and convert them to specific CNC-understandable internal structure code for the execution purpose. It is one of the critical modules that reflect the system performance straightly. However, conventional CNC controllers are considered as closed to nature and manufacturer's specification dependency. Thus, advanced technologies cannot be implemented in the current CNC controller directly. For improve the universality, portability, modularity, interoperability and expansibility on the next generation of adaptive CNC controller, a new model of the CNC program interpreters is proposed based on layered CNC-Function Block architecture.

1. INTRODUCTION

In the conventional system, computer numerical control (CNC) cannot execute directly based on a numerical control (NC) program that is developed by a computer-aided manufacturing (CAM) system. The CNC program must be converted into particular CNC-understandable internal structure code such as motion command and programmable logic controller (PLC) commands via the interpreter module. Therefore, interpreter is one of the critical modules that reflect the CNC system performance straightly. However, with the progressive growth of NC technology, conventional CNC systems are limited with the interpreter lacking in expansibility, modularity, and openness [1].

Today, multiple CNC controller brands with the variety of capabilities are employed by the industries to fulfill customer requirement. The majority of them use ISO 6983 (also known as G&M code) as a data interface between CAD/CAM and CNC as presented in Figure 1. However, due to the limited scope of ISO 6983, there are a lot of non-standard extended available in the market that adapts their own specific function [2]. Besides that, there are various of problems found in this data interface such as: delivering limited information to CNC, unidirectional data transfer from CAD/CAM to CNC, unable to provide seamless integration between the Computer-Aided system (CAx) [3]. But, in reality, these G&M code programs are very valuable because they incorporate both an implicit micro process plan as well as many years of operator experience [4]. For this reason, a function for interpreting G&M code is included in this system as well.

STEP-NC (ISO 14649) is a new ISO model for data transfer in the CAx. STEP-NC is extended STEP (ISO 10303) for numerical control. It remedies the shortcomings of G&M code by specifying machining processes rather than the machine tool motion, using the object-oriented concept of working steps, as a basic entity [5]. As a standard contains comprehensive information model, STEP-NC provides seamless integration among CAx system without any information loss. Moreover, it makes the CNC more open, interoperable and intelligent. Thus, a smart intelligent CNC controller that is responsible for translating working steps, instead of G&M codes for executing the CNC machine is required. These STEP-NC compliant CNC controllers are destined to evolve from pure controllers into integrated systems with both decision-making and control abilities [6]. Therefore, this new controller should be able to make decisions about the process specific decision such as automatic and optimal tool path generation.

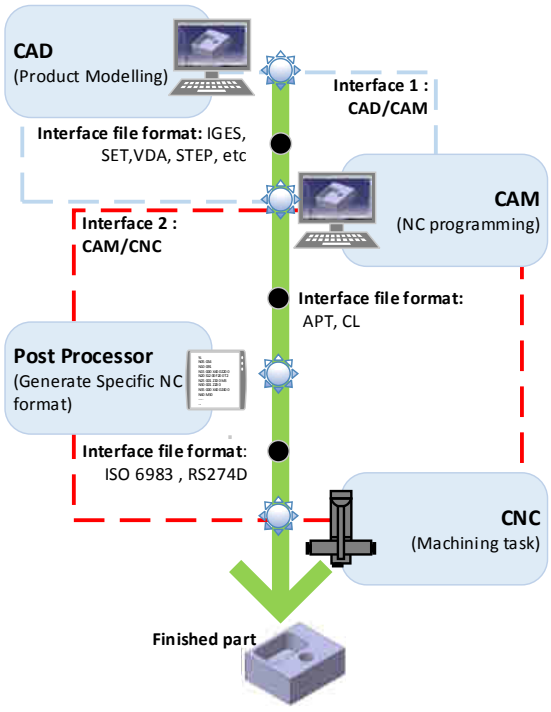

Figure 1 CAx data model interface

To date, a number of researchers have reported different approaches to enhance capabilities of the CNC controller system as well as their interpretation

techniques, and some of them are present in Table 1. The aim of this technology is to build controllers independent of any vendor technology and can receive more than one data model as their input. In this paper, a new technique is presented in the interpretation of the ISO 6983 and ISO 14649 data interface model.

Table 1 Previous research

Researcher	Year	Interpretation module
Yusof, Y. & Latif, K. [1]	2015	ISO 6983 and ISO 14649 into internal machine structure
Shin, S.J et al [4]	2007	ISO 6983 into ISO 14649
Xu, X.W. [7]	2006	ISO 14649 into 6K program

2. METHODOLOGY

The proposed methodology for interpreting the NC program focuses on the use of STEP-NC standard as a data model interface for the system. The system incorporates STEP-NC with layered IEC 61499 function blocks (FBs) technology as presented in Figure 2. It can take ISO 6983 and STEP part 21 program file as an input. The interpreter system is developed using the proposed language and in the JAVA environment. This interpreter device is supported with the Graphic User Interface (GUI) for providing easy, efficient, and user-friendly characteristics.

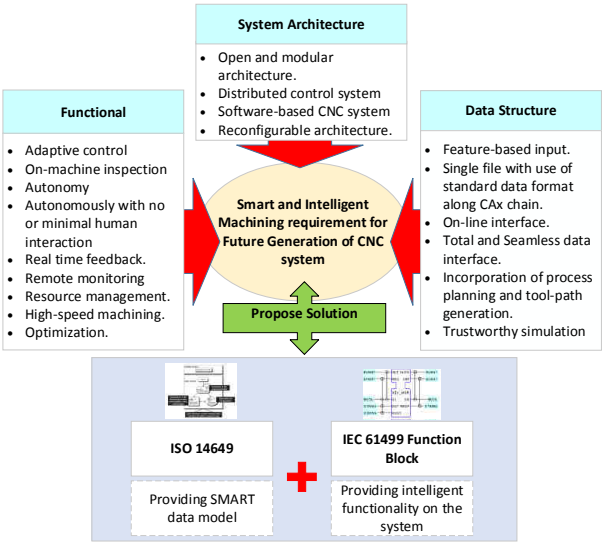

Figure 2 Smart and intelligent machining requirement

3. RESULT AND DISCUSSION

The outcome of this research project is a plug-and-play software program called Adaptive STEP-NC/FB Interpreter device, which is competent enough to interpret STEP-NC (Part 21) program files and ISO 6983 program files as presented in Figure 3. The layered FB architecture is proposed to simplify the design of interpreter device. In the proposed system, a user needs to select the interpretation module based on input data. Then, the input file is transferred to the abstraction and mapping module for extracted all the related machining processing data and then the extracted data will be combined into new single code. Output data model then forwards the translated code to open CNC machine for operations as shown in Figure 4.

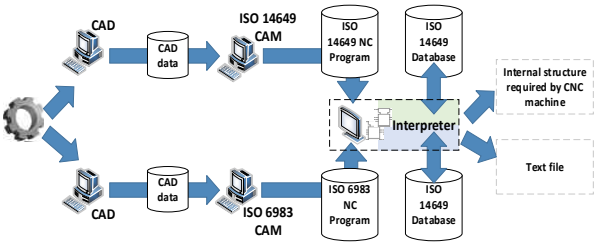

Figure 3 Conceptual design of developed module

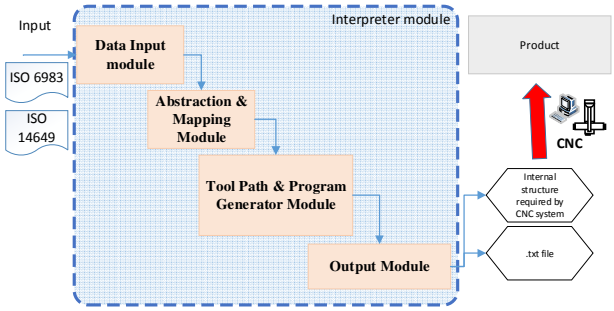

Figure 4 Working principle of the interpreter module

4. CONCLUSIONS

In this work, STEP-NC/FB interpreter is proposed to interpret NC program (ISO 6983 and STEP-NC) into generic STEP-NC representation. Later, this generic representation can be used to re-generate part program for specific controller. The layered STEP-NC/FB architecture is proposed as to simplify the design of interpreter and provides flexibility in adopting the interpreter in new systems or modification in the future.

REFERENCES

[1] Y. Yusof and K. Latif, "New Interpretation Module for Open Architecture Control Based CNC Systems," *Procedia CIRP*, vol.26, pp.729–734, 2015.

[2] S. Xú, N. Anwer, and S. Lavernhe, "Conversion of G-code programs for milling into STEP-NC," in *International Joint Conference on Mechanics, Design Engineering and Advanced Manufacturing, Toulouse, France 2014*, 2014, pp. 495.

[3] S. H. Suh and S. U. Cheon, "A framework for an intelligent CNC and data model," *Int. J. Adv. Manuf. Technol.*, vol.19, no. 10, pp.727–735, 2002.

[4] S.-J. Shin, S.-H. Suh, and I. Stroud, "Reincarnation of G-code based part programs into STEP-NC for turning applications," *Comput. Des.*, vol. 39, no. 1, pp. 1–16, 2007.

[5] X. . Xu and Q. He, "Striving for a total integration of CAD, CAPP, CAM and CNC," *Robot. Comput. Integr. Manuf.*, vol.20, no. 2, pp.101–109, 2004.

[6] C. Zhang, R. Liu, and T. Hu, "On the futuristic machine control in a STEP-compliant manufacturing scenario.," *Int. J. Comput. Integr. Manuf.*, vol. 19, no. 6, pp. 508–515, 2006.

[7] X. W. Xu, "Realization of STEP-NC enabled machining," *Robot. Comput. Integr. Manuf.*, vol. 22, no. 2, pp. 144–153, 2006.

Parameter-magnitude based information criterion for identification of linear discrete-time model

M.F.A.Samad*, A.R.M.Nasir

Faculty of Mechanical Engineering, Universiti Teknikal Malaysia Melaka (UTeM), 76100 Durian Tunggal, Melaka

*Corresponding e-mail: mdfahmi@utem.edu.my

Keywords: Information criterion, system identification, discrete-time model

ABSTRACT – Information criterion is an important factor for model structure selection in system identification. It is used to determine the optimality of a particular model structure with the aim of selecting an adequate model. This paper introduces a new parameter-magnitude based information criterion (PMIC2) for identification of linear discrete time model. It is shown that PMIC2 is able to select a suitable model in linear discrete-time model.

1. INTRODUCTION

System identification can be defined as approximating a dynamic system models using experimental data [1]. Its basic idea is to compare the time dependent responses of the actual system and identified model based on a performance function, hereby referred to information criterion, giving a measure of how well the model response fits the system response [2].

Model complexity selection is the sub-problem of model selection [3]. Parsimony, working hypotheses, and strength of evidence are three principles that regulate the ability to make inferences [4]. A model accuracy and model parsimony known as variance and bias: $f(J) = Var(J) + Bias(J)$ is an important consideration in selecting a model structure [5]. Hence, selecting a model with smallest variance is not a good idea because when the number of parameters increase, the variance will continue to decrease but will present a complex model. At a certain complexity, the additional parameters no longer reduce the systematic errors but are used to follow the actual noise realization on the data [6].

Often, in order to deal with the bias-variance trade-off, the information criterion is augmented with a penalty term intended to guide the search for the "optimal" relationship penalizing undesired regressors, where regressors refer to possible terms and variables identified from model order and linearity specifications. Regularized estimation has been widely applied also in the context of system identification [7].

In this paper, the effectiveness of parameter-magnitude-based information criterion will be studied by testing three simulated dynamic models in the form of difference equations model. These models are linear autoregressive models with exogenous input (ARX) [8]. The benefit of using simulated models is the presence of an opportunity to compare the final model directly with the true model.

2. METHODOLOGY

The methodology is to develop further the approach of using parameter magnitude information in information criterion [5, 9]. It includes a bias term or known as penalty function and here will be denoted as PMIC2. The PMIC2 then will be used for model structure selection of discrete-time system. The selected model structure will be compared with correct/simulated model structure.

The PMIC2 can be written as:

$$\sum_{n}(y(t) - \hat{y}(t))^2 + \sum_{j}\frac{1}{\theta_j}$$

Where $y(t)$ is the actual output, $\hat{y}(t)$ is the k-step-ahead predicted output, θ_j is the magnitude of parameter in the model and j is the number of parameter.

The research implementation steps are:

1. To develop the PMIC2 based on the finding of the previous study.
2. To generate simulated data in the data acquisition stage
3. To apply and calculate the performance of PMIC2.
4. To analyse the effectiveness of PMIC2 by comparison of the selected model with true model.

3. SIMULATION SETUP

In this simulation, three ARX models are simulated using computer simulation software MATLAB. All models are denoted as Model 1, Model 2, and Model 3 and each model is further classified as having d.c. level. The following are the models written as linear regression models, its specifications, number of correct regressors and number of possible regressors:

Model 1:

$$y(t) = 0.2y(t-2) + 0.5u(t-1) + 0.8u(t-3) + e(t)$$

Specification: l=1, assumed maximum output order, n_y=3, assumed maximum input order, n_u=3.
Number of correct regressor = 3 out of 7
Number of possible model =127

Model 2:

$$y(t) = 0.1y(t-2) - 0.4y(t-4) + 0.5u(t-1) + 0.7u(t-3) + e(t)$$

Specification: l=1, assumed maximum output order, n_y=4, assumed maximum input order n_u=4
Number of correct regressor = 4 out of 9

Number of possible model =511
Model 3:

$$y(t) = 0.2y(t-2) - 0.3y(t-4) + 0.6u(t-1) + 0.8u(t-5) + e(t)$$

Specification: l=1, assumed maximum output order, n_y=5, assumed maximum input order n_u=5
Number of correct regressor = 4 out of 11
Number of possible model = 2047

4. RESULTS AND DISCUSSION

In this section, comparison is made between the selected model of PMIC2 and simulated model. From the simulation result, the PMIC2 can select the same model as true model for all simulated models. Table 1 shows the value of PMIC2 for variance term, bias term and total for both terms. Note that the minimum value of PMIC2 among models become the selected model.

Table 1 The value of PMIC2

Models	Variance	Bias	Total
Model 1	0.21830	8.20378	8.42209
Model 2	0.19912	15.95503	16.15416
Model 3	0.18292	11.22241	11.40533

As can be seen, the bias value is bigger than variance value for all models. Variance and bias is inversely proportional, when variance value is small, the bias value is big and vice versa. Despite this, a fine balance between the two enables PMIC2 to select the model which is the same as the given model.

5. CONCLUSIONS

From the observation, the PMIC2 proved that it can perform well when selecting a correct model in linear discrete time model. However, it had not been tested yet on non-linear model. Further study will be concentrated on non-linear autoregressive models with exogenous input (NARX).

ACKNOWLEDGEMENT

Authors are grateful to Universiti Teknikal Malaysia Melaka and Ministry of Higher Education Malaysia for the financial support through grant FRGS/1/2015/TK03/UTeM/02/16.

REFERENCES

[1] A. Saleem, B. Taha, T. Tutunji, and A. Al-Qaisia, "Identification and cascade control of servo-pneumatic system using particle swarm optimization," *Simul. Modell. Pract. Theory*, vol. 52, pp. 164-179, 2015.

[2] A. Alfi, and M. M. Fateh, "Parameter identification based on a modified PSO applied to suspension system," *J. Software Eng. Appl.*, vol. 3, pp. 221-229, March 2010.

[3] K. Kristinsson and G. A. Dumont, "System identification and control using genetic algorithms," *IEEE Trans. Syst. Man Cybern.*, vol. 22, pp.1033-1046, 1992.

[4] L. Xiaoyong, F. Huajing and C. Zhaoxu, "A novel cost function based on decomposing least-square support vector machine for Takagi-Sugeno fuzzy system identification," *IET Control Theory Appl.*, vol. 8, pp. 338-347, 2013.

[5] M.F. Abd Samad, H. Jamaluddin, R. Ahmad, M.S. Yaacob and A.K.M. Azad, "Effect of penalty function parameter in objective function of system identification," *Int. J. Automot. Mech. Eng.*, vol. 7, pp. 940-954, 2013.

[6] F. D. Ridder, R. Pintelon, J.Schoukens, and D. P. Gillikin, "Modified AIC and MDL model selection criteria for short data records," *IEEE Trans. Instrum. Meas.*, vol. 54, pp. 144-150, 2004.

[7] G. Prando, G. Pillonetto and A. Chiuso, "The role of rank penalties in linear system identification," *IFAC-Papers online*, vol. 48, pp. 1293-1300, 2015.

[8] L. Ljung, *System Identification: Theory for the User*, 2nd ed., Prentice Hall, Upper Saddle River, 1999.

[9] M.F.A. Samad and A.R.M. Nasir, "Comparison of Information Criterion on Identification of Discrete-Time Dynamic System". *Int. J. Eng. Technol.* To be published.

Tool entry impact on bobbin friction stir welding quality

M. K. Sued [1,*], F. A. R. Fadil[2], M.R. Ramli[2], B. Abu Bakar[1]

[1)] Advanced Manufacturing Centre, Faculty of Manufacturing Engineering, Universiti Teknikal Malaysia Melaka, Hang Tuah Jaya, 76100 Durian Tunggal, Melaka, Malaysia
[2)] Faculty of Manufacturing Engineering, Universiti Teknikal Malaysia Melaka, Hang Tuah Jaya, 76100 Durian Tunggal, Melaka, Malaysia

[*]Corresponding e-mail: kamil@utem.edu.my

Keywords: Friction Stir Welding; Bobbin tool; Aluminum

ABSTRACT – Bobbin Friction Stir Welding (FSW) process has the benefits of the conventional friction stir welding (CFSW) but at a greater level. Besides, the defects of common traditional welding methods such as cracking and distortion have been eliminated, the process runs at low energy consumption, high heat generation and required less fixture demand. However, it is found that tool entry is challenging, especially for fixed type of bobbin tool. This is because the material to be welded needs to be located between the shoulders, thus limiting the flexibility of the process and eventually affects the quality of the weld. Therefore, in this early work, process difficulty is measured through current consumption of the spindle motor of different tool entry approaches. It is found that guided hole tool entry consume higher energy compared to the edge entry.

1. INTRODUCTION

Friction stir welding technology (FSW) as shown in Figure 1 involves a solid-state bonding by a non-consumable tool that rotates and mechanically travels through the work-pieces to be joined. Tool rotation generates heat for material softening and closes the weld behind. The technology has been applied to shipbuilding, automotive and aerospace industries [1, 2]. It represents an alternative welding technology process over fusion welding, e.g. tungsten inert gas welding (TIG) and metal inert gas welding (MIG). These traditional joining techniques require close process monitoring, high energy consumption and labor involvement, and potentially provide poorer welded joints which require post processing work.

There are two fundamental types of FSW technology, based on the tool features: single and twin flanges. The single sided tool or CFSW, as the name suggests, has only a single flange, and it engages with only one side of the substrate. This tool design is the main one used in the field, and dominates the research literature. It has a potential for incomplete root penetration, unless additional effort is taken with backing plates or two-sided welds, hence is suitable for joining thicker materials. In contrast the twin-flanged tool, which is shaped like a bobbin, hence BFSW, locates a flange at both sides of the substrate. The idea is that this generates more heat and better process-setup than the CFSW. In principle, this might be a better tool to use in industry, but adoption has been slow as there are a number of difficulties with the bobbin design.

The issue is that there are numerous variables that affect weld quality. The relationships between variables, and their effects on quality, are complex and not fully understood. This will impact the selection of the process parameters as shown by previous studies that different process parameters have been suggested for welding similar materials [4, 5]. An early study of these interactions in revealing the relationship between variables has been done by Sued et al [6, 7]. However, a focus should be given to tool entry since material to be welded needs to be in the obtainable region of the tool to stir. This is for pressure, heat and material relocation before diffusion process. This has not been the case of CFSW because of the absent of bottom shoulder hence, easy on the tool entry strategy. Parameters such as plunge force, tilting angle, shorter tool pin and tab run in ascertaining the material to be around the tool for stirring. For BFSW, the bottom shoulder limits the tool entry flexibility. Because of this, it is believed that the defects such as tunnel can be generated. In this study, two methods for tool entry are used, which are guided hole and edge entry. Current signal of the spindle motor is measured to assess the work delivered by the tool.

2. METHODOLOGY

To access the impact of tool entry on the energy demand of the BFSW process, two types of tool entries were conducted. They were guided hole and edge entry as illustrated in Figure 1. For the guided hole entry, plate was assembled around the tool before tool rotation and for the edge entry, the rotated tool was passed through the materials from the edge. The weldings were piloted on the 3 axis CNC milling machine having 20-horsepower capability. Material to be welded was aluminum 3000 series with the size of 140mm x 140mm x 6 mm (thickness). The tool used was a fixed type with the features of flat shoulder and cylinder pin. A compression ratio as recommended in [8] was used. The material of the tool was hardened tool steel H13 type. Current was measured using digital power clamp meter UT235. The measurement was conducted at the CNC spindle motor. The welding process parameters were 700rpm and 310 mm/min for the spindle and feed rate speed, respectively. Besides, graph of current (A) versus time (s) was plotted to observe the weld formation. The welded plates were also tested on crack and void defects using non-destructive test dye penetrant type.

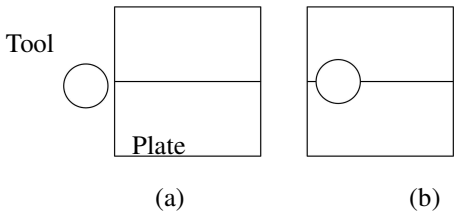

Figure 1: Tool entry approaches: (a) Edge entry, (b) Guided hole entry.

3. RESULTS AND DISCUSSION

All produced welds are free form any void, holes and crack types of defect. As clearly seen in Figure 2(a), , a volume of materials has been ejected away from the plate forming a 'rooster head' shape in edge entry approach. Meanwhile, an amount of material has been removed during hole preparation for the guided hole entry approach (Figure 2(b)). This is because for the solid tool to be positioned inside the plate, some materials need to be removed.

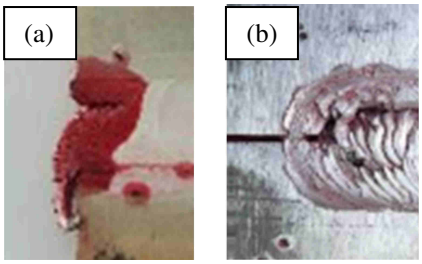

Figure 2: Photographic images of (a) Edge entry and (b) Guided hole entry.

Figure 3 shows the current versus time graph. The diagram represents consumed energy for both tool entries. It is clearly shown that guided hole consumed more energy (about 2A higher) than the edge entry. The reason is because of the presence of hard material around the tool when the tool starts to rotate. For the edge entry, the fluctuation of current is started when the tool touches the edge at slow feed and only pickup at welding speed. The material ahead of the tool is in *readiness condition* due to heat transfer.

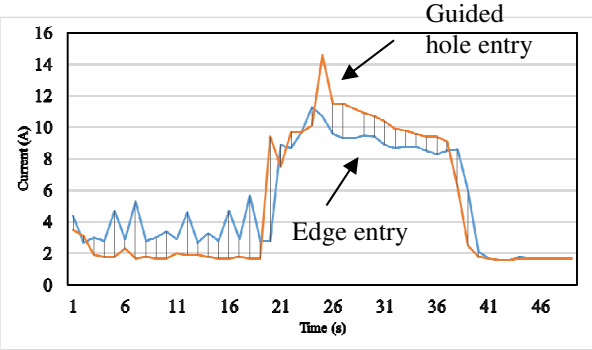

Figure 3: Current consumption at the tool entry.

4. CONCLUSIONS

The study presents the impact of different tool entry approaches. Guided hole entry is found to consume more current in order to break the hard material whereby for the edge entry the ahead material is already in the readiness condition, hence less energy is required. Although both entries did not produce any surface defects, further study on cross-section is required. It is believed that material availability around the tool especially after the ejection can cause material limitation for stirring and tunnel defect to occur. It is believed this condition is more crucial in thin material (below 6 mm thickness). However, from this work it can be concluded that less energy is required to stir the material that in readiness condition which is the case of edge entry.

ACKNOWLEDGEMENT

Authors are grateful to Universiti Teknikal Malaysia Melaka for the financial support through PJP grant numbered PJP/2016/PROTON/FKP-AMC/ S01503.

REFERENCES

[1] I. Bordesoules, A. Bigot, C. Hantrais, T. Odievre, and J. Laye, "Aircracts Structural Parts Demonstrators Manufactured Using Friction Stir Welding," presented at the 9th International Symposium on Friction Stir Welding, Huntsville, USA, 2012.

[2] J. Carstensen and J. F. Dos Santos, "Application of FSW and FSSW on Advanced Automotive Structural Applications," presented at the 9th International Friction Stir Welding Symposium, Huntsville, USA, 2012.

[3] P. L. Threadgill, M. M. Z. Ahmed, J. P. Martin, J. G. Perrett, and B. P. Wynne, "The use of bobbin tools for friction stir welding of aluminium alloys," *Thermec 2009, Pts 1-4*, vol. 638-642, pp. 1179-1184, 2009.

[4] K. J. Colligan, A. K. O'Donnell, J. W. Shevock, and M. T. Smitherman, "Friction Stir Welding of Thin Aluminium Using Fixed Gap Bobbin Tools," presented at the 9th International Symposium of Friction Stir Welding, Von Braun Center, Huntsville, Alabama, USA, 2012.

[5] H. J. Liu, J. C. Hou, and H. Guo, "Effect of welding speed on microstructure and mechanical properties of self-reacting friction stir welded 6061-T6 aluminum alloy," *Materials & Design,* vol. 50, pp. 872-878, 2013.

[6] M. K. Sued, D. Pons, J. Lavroff, and E. H. Wong, "Design features for bobbin friction stir welding tools: Development of a conceptual model linking the underlying physics to the production process," *Materials & Design,* vol. 54, pp. 632-643, 2014.

[7] M. K. Sued and D. Pons, "Dynamic interaction between machine, tool, and substrate in bobbin friction stir welding (*Accepted for publication*)," *Journal of Manufacturing Engineering,* 2016.

[8] M. K. Sued, D. Pons, and J. Lavroff, "Compression Ratio Effects in Bobbin Friction Stir Welding," in *10th International Friction Stir Welding Symposium*, Beijing, China, 2014.

Effect of reflow cycle on the shear strength of Sn-3.5Ag/Ni-P/EFTECH 64-Ni, EFTECH 64-Cu and C194-Ni bump

C.G.Ong[1,2,*], K.T.Lau[2]

[1)] Infineon Technologies (Malaysia) Sdn. Bhd., Melaka, Malaysia

[2)] Faculty of Manufacturing Engineering, Universiti Teknikal Malaysia Melaka, Hang Tuah Jaya, 76100 Durian Tunggal, Melaka, Malaysia

[*]Corresponding e-mail: daniel.ong@infineon.com

Keywords: Electroless nickel, shear strength, Cu alloy carrier

ABSTRACT – Shear strengths of the Sn-3.5Ag/Ni-P solder joint on the EFTECH 64-Ni, EFTECH 64-Cu and C194-Ni carrier-bumps underwent different reflow cycles were examined. The reflow cycles were controlled at soldering temperatures of 240 and 260°C, and reflow times of 5, 10, 20 and 30 minutes. Under extended reflow cycle and high reflow temperature have significant influences on interfacial compounds (IFCs) solder joint considerably. The design of experiment (DOE) input factors on Cu alloy were established with the help of Cornerstone Software. EFTECH 64- and C194-Ni bump resulted consistency in their repeatability in shear strength test compare to EFTECH 64 Cu bump.

1. INTRODUCTION

Mechanical reliability of the solder joint connected to the Electroless Nickel Immersion Gold (ENIG) surface of the interconnection bump is critical in electronic package qualification [1]. Performance of Ni based under bump metallization's (UBMs) are preferred than the Cu based, due to the advantages such as low commercial cost, uniform deposition, excellent solderbility and corrosion resistance [1-2]. The reaction between the Sn solder and Ni-P formed a strong solder joint [3], and produces three layer of interfacial compounds, Ni_3Sn_4, Ni-Sn-P, and Ni_3P [2]. Previous studies are focusing on the mechanical reliability of Ni-P/solder interfacial on different bond pads [1-5]. Thin ternary Ni-Sn-P layer grows between the Ni_3Sn_4 and Ni_3P after reflow process influences the solder joint strength [1].

However, the previous findings on the main cause of the deterioration in shear strength of electroless Ni-P/solder joint is still not conclusive. Thus, this work attempts to investigate three main factors which have predominant influence on the shear strength of the electroless Ni-P/solder joint. The three factors are Cu alloy carrier-bump combination, reflow time and reflow temperature.

2. METHODOLOGY

Assemblages of Ni- or Cu-bumps on the copper alloy carrier (EFTECH-64 or C194 grade) were obtained from the supplier. After the bump-carrier assemblage was encapsulated with free halogen mold compound, the Cu alloy carrier was etched away by a $CuCl_2$ etchant to expose the bumps. Next, the exposed bumps' surface was plated with electroless Ni-P with thickness of 4.5 um using a commercial Electroless Nickel (EN) solution. For the Cu bump surface, an activator was used to initiate the Ni-P deposition. The surface finishing of the Ni-P bumps was coated with Au coating (thickness ~ 0.08 μm) by the immersion gold (IG) plating for oxidation resistance purpose.

After the plated bump was coated with Sn-3.5 Ag solder paste (flux dipping), the whole molded package was mounted on printed circuit board (PCB) at the bump's positions. The assembly underwent reflow oven to increase or form solder joints in between Ni-P/Sn-3.5Ag layer. Finally, shear strength test was performed on the PCB-mounted mold package at room temperature. A full factorial design of experiment (DOE) with total runs of 24 ($=2^1 \times 4^1 \times 3^1$) of the shear strength data were analyzed using CEDA software. Details of the related input factors are tabulated in Table 1.

Table 1 Investigated factors and levels.

Factors	Units	Type	Levels
Reflow time	min	Numeric	2
Reflow temperature	°C	Numeric	4
Cu alloy carrier-Bump	N/A	Category	3

3. RESULTS AND DISCUSSION

3.1 DOE Analysis and Optimization

The DOE data has a model's goodness fit in terms of R-squared = 89.86% and adjusted R-squared 88.64% at 99% confident level. Interaction test results between the investigation factors and shear strength showed positive interactions with the reflow temperature and reflow time. Furthermore, the EFTECH 64-Cu samples showed low shear strength value compare to C194-Ni and EFTECH 64-Ni. Whereas, both C194-Ni and EFTECH 64-Ni comparable in all parameter magnitude.

In order to archive consistency in shear strength value, an optimization by Cu alloy carrier was computerized with reflow parameter factor using Cornerstone Software. In this optimization process, materials were replicated to understand the best setting for it. Each Cu alloy carrier has specific parameter in order to achieve low standard deviation and high shear strength value [7-8]. Optimization of EFTECH 64-Ni and C194–Ni bump reflow parameter are comparable to

each other but EFTECH 64-Cu have stand-alone reflow parameter in order to archived low standard deviation and shear value more than 900 gmf.

Table 2 Proposed reflow parameters the Sn-3.5Ag/Ni-P solder joint at different Cu alloy carriers.

Cu alloy Carrier-Bump	Reflow temperature, °C	Reflow time, min	Std. Dev*
C194-Ni	250	7.3	275.3
EFTECH 64-Ni	249	6.9	264.1
EFTECH 64-Cu	258	18.3	555.3

Note: Std.Dev = Standard Deviation.

3.2 Comparison between EFTECH 64-Ni, EFTECH 64-Cu and C194-Ni bump.

Small bias and high robustness at optimal variable setting are desirable properties to obtain small range of shear strength standard deviation within Cu alloys carrier at 99% confident level. p-value of the shear strengths' standard deviations showed no significant difference between C194-Ni and EFTECH 64-Ni bump assemblages. However, significant p-value between C194-Ni and EFTECH 64-Cu, and between EFTECH 64-Ni and EFTECH 64-Cu bumps at different reflow factors. The proposed reflow parameters of EFTECH 64-Cu (Tables 2) and standard deviation (Tables 3) indicated that a stable and consistency of shear strength can be achieved at 260 and 240°C in 30 min and 20 min respectively.

Table 3 Standard deviations of shear strength of carrier-bump assemblage at different reflow cycles.

Reflow Temperature, °C	Reflow Time, min	C194-Ni/ EFTECH 64-Ni	C194-Ni/ EFTECH 64-Cu	EFTECH 64-Ni/ EFTECH 64-Cu
240	5	0.6118	0.0234	0.0698
	10	0.9342	0.0255	0.0306
	20	0.8556	0.0465	0.0313
	30	0.6459	0.0814	0.1898
260	5	0.6034	0.0159	0.0508
	10	0.3359	0.0017	0.0189
	20	0.9222	0.0924	0.0763
	30	0.6273	0.0090	0.0026

Intermetallic (IMCs) thicknesses of EFTECH 64-Cu/electroless Ni-P/Sn2.5Ag at proposed parameter are comparable with C194-Ni and EFTECH 64-Ni IMCs thicknesses. IMCs thicknesses of solder joint increased at different reflow temperature and time, but will decrease the growth rate as increase in reflow time [4, 6]. Besides, at optimum reflow parameter, consistency of shear strength standard deviation and no Ni-P/Cu layer separation was observed. However, after peak reflow time at 20 min in 260°C, inconsistency shear strength between Cu alloys carrier was observed. Brittle solder joint occurred after the depletion of crystallized Ni_3P /Cu layer due to void formation [1, 4].

4. CONCLUSION

In different reflow temperature and time, correlation of IMCs growth can be observed through shear strength consistency. Finally, it is clear that EFTECH 64-Cu required high temperature (258 °C) and longer time (18.3 min) compare others Cu alloy carrier.

5. REFERENCES

[1] A. Kumar, and Z. Chen, "Effect of Ni-P thickness on the tensile strength of Cu/Electroless Ni-P/Sn-3.5Ag solder joint," *IEEE Transactions on Components and Packaging Technologies*, vol. 29, pp. 886-892, 2006.

[2] Mona, A. Kumar, and Z. Chen, "Influence of Phosphorus content on the interfacial microstructure between Sn-3.5Ag Solder and Electroless Ni-P Metallization on Cu substrate," IEEE Transactions on Advanced Packaging, vol. 30, no. 1, pp. 68-72, 2007.

[3] C. Y. Ho, and J. G. Duh, "Optimal Ni-P thickness design in ultrathin ENEPIG metallization for soldering application concinnity electrical impedance and mechanical bonding strength," *Material Science and Engineering: A*, vol. 611, pp. 162-169, 2014.

[4] L. Zhang, C. Andersson, J. Liu, and Z. Cheng, "The effect of reflow temperature and time on the formation and growth kinetics of intermetallic compound (IMCs) between Sn-0.7Cu-0.4Co Eutectic solder and ENIG/Cu Substrate finish," in *2nd Electronics Systemintegration Technology Conference 2008*, 2008, pp. 1296-1300.

[5] Z. Huber, J. W. Budka, A.W. Miernik, A. Sypien, M. Szczerba, and P. Zieba, "Influence of Phosphorous content on microstructure development at the Ni-P/SAC Interface," *Electronic Material Letter*, vol. 12, no. 1, pp. 178-185, 2016.

[6] M. O. Alam, Y.C. Chan, and K.N. Tu, " Effect of rection time and P content on mechanical strength of the interface formed between eutectic Sn-Ag solder and Au/electroless Ni(P)/Cu bond pad," *Journal of Applied Physics*, vol. 94, no. 6, pp. 4108-4115, 2003.

[7] C. G. Ong, K. T. Lau, M. Zaimi, M. Afiq, & K. P. Queck, "Effect of electroless Ni-P thickness on EFTECH 64-Ni, EFTECH 64-Cu and C194-Ni bump," in *Microsystems, Packaging, Assembly and Circuits Technology Conference (IMPACT) 2016 11th International*, 2016, pp. 319-322.

[8] C. G. Ong, K. T. Lau, M. Zaimi, K. S. Goh, & M.Q. Tay, "Effect of Cu based complexes on EFTECH 64 and C194 Cu alloy," in *Electronics Manufacturing Technology (IEMT) & 18th Electronics Materials and Packaging (EMAP) Conference, 2016 IEEE 37th International*, 2016, pp. 1-4.

Proceedings of Innovative Research and Industrial Dialogue'16, pp. 135-136 (May 2017)

The dynamic verification of vehicle roll dynamic models using different software's

F.M. Jamil[1], M.A. Abdullah[1,2,*], M. Ibrahim[1], M.H. Harun[1,2], W.M.Z. Wan Abdullah[1,2]

[1)] Faculty of Mechanical Engineering, Universiti Teknikal Malaysia Melaka, Hang Tuah Jaya, 76100 Durian Tunggal, Melaka, Malaysia
[2)] Centre for Advanced Research on Energy, Universiti Teknikal Malaysia Melaka, Hang Tuah Jaya, 76100 Durian Tunggal, Melaka, Malaysia

[*]Corresponding e-mail: mohdazman@utem.edu.my

Keywords: Vehicle roll model, suspension system, vehicle ride

ABSTRACT – In an automotive industries, suspension system plays an important role to bear the vehicle weight, to cut off the vehicle body from road disturbances and to preserve the traction force between the tire and the road surface. However, the ride comfort is the main concern for the passengers during vehicle operating conditions. This paper focuses on the analysis and verification of vehicle roll model of passive suspension system. The model is developed using Matlab/Simulink and vehicle data from CarSim software is used in the simulation. The relations among parameters and vehicle roll dynamics are determined and established. The vehicle roll model is verified by the CarSim software.

INTRODUCTION

Ride and handling are one of the key attributes in the vehicle, which communicate directly to the customer perception of satisfaction. Thus, the need for passenger comfort, road handling abilities of tires, vehicle handling characteristics, have been the major challenge in the design of suspension system over the years. Nowadays, anti-roll systems have been develop and widely studied in automotive industry. The proposed of this system is to increases the controllability of the vehicle, by giving access to the roll angle which is usually uncontrollable. Active anti-roll system allowing the control of the roll angle and thus improving the vehicle stability, especially when turning or when moving on slopping ground [1, 2]. Moreover, the rollover accidents induced by severe maneuvers are very dangerous and mostly happen to vehicles with elevated center of gravity. Unfortunately, it is hard for drivers of those vehicles to predict and prevent the trend of the maneuver-induced (untripped) rollover ahead of time [2]. In addition, vehicle roll motion occurs when a vehicle is turning on its horizontal axis. This is due to lateral acceleration and low normal force on inner wheels. Besides, under critical driving conditions such as emergency cornering, it is normally difficult for a driver to stabilize the vehicle, and accidents can occur in such critical driving situations [3]. To ensure vehicle active safety performance, many advanced active chassis control systems like active front steering, direct yaw moment control (DYC) and active roll control (ARC) system, have been developed and brought into the market [4].

METHODOLOGY

In this analysis, the verification has been made on rolling performance between Simulink model and the simulation using CarSim software (Figure 1). The parameters used in this analysis has been taken from CarSim simulation as in Table 1, while the model (Figure 2) has been developed using Matlab/Simulink software. The value of body vertical acceleration (az) and roll angular displacement (phi) needed to be determined and verified. Figure 2, shows a free body diagram (FBD) of 4 degree of freedom (DOF) vehicle roll model. The equations of motion have been developed with referred to the FBD and the modelled using Simulink/Matlab software [5].

Figure 1 Simulation roll car model from CarSim

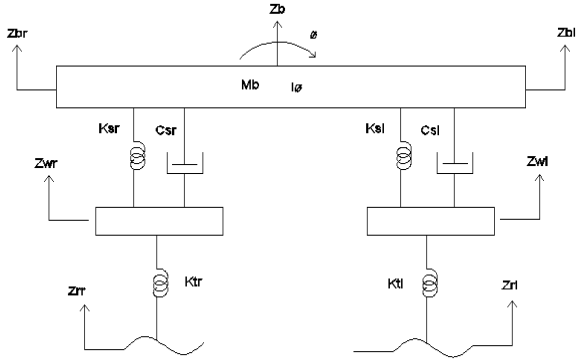

Figure 2 Vehicle roll model

Table 1 Vehicle parameters

Symbol	Description	Value
m_b	Kerb Weight	1653kg
c_{sr}	Right Damper stiffness	30kNs/m
c_{sl}	Left Damper stiffness	30kNs/m
k_{sr}	Right Spring Stiffness	34kN/m
k_{sl}	Left Spring Stiffness	34N/m
k_{tr}	Right Tire Stiffness	230kN/m
k_{tl}	Left Tire Stiffness	230kN/m
m_{wr}	Right wheel unsprung mass	90kg
m_{wl}	Left wheel unsprung mass	90kg
i_ϕ	Inertia in Yaw direction	614kg/m^2
t	Track	1.6m

RESULT AND DISCUSSION

From outcomes of the results obtained in Figure 3 and Figure 4, the trends between model and simulation are identical and come with small error. Overall reading of angular displacement follows the same pattern of between model and simulation data. These show that the vehicle dynamic roll model developed using Matlab/Simulin is verified by CarSim software.

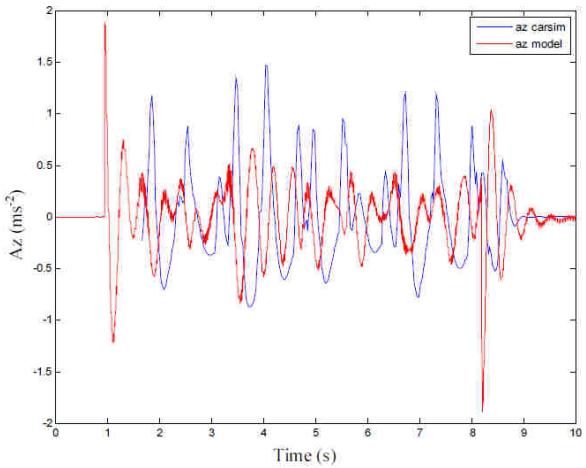

Figure 3 Vehicle vertical vibration

CONCLUSION

For a conclusion, the model graph follow the same pattern of simulation graph. There are several of misalignments of the pattern at some point on the graph but the system mostly follow the pattern from CarSim. Overall, the model is verified since there is a consistent pattern between simulation and model. Moreover, vehicle system such as a suspension system has influenced the vehicle movement in order to avoid unnecessary body displacements and accelerations which acting on the vehicle. It's also give the passengers comfort while handling. This verified model can be further used for evaluation of dynamic performance and active safety rollover prevention.

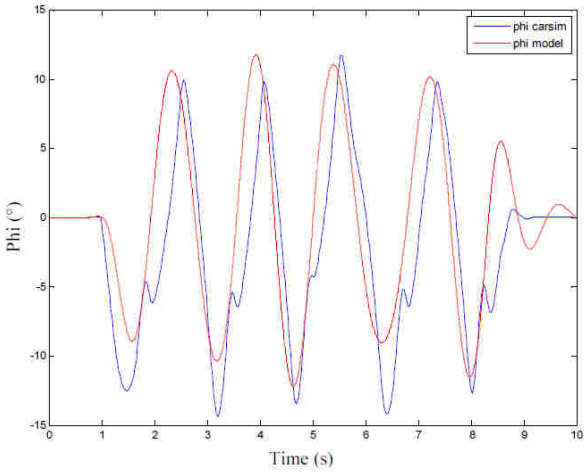

Figure 4 Vehicle roll motion

ACKNOWLEDGEMENT

The authors gratefully acknowledged the Advanced Vehicle Technology (AcTiVe) research group of Centre for Advanced Research on Energy (CARe), the financial support from Universiti Teknikal Malaysia Melaka, PTPTN and The ministry of Education, Malaysia under Short Term Research Grant, Grant no. PJP/2014/FKM(10A)/S01330 and Fundamental Research Grant Scheme (FRGS), grant no.: FRGS/2013/FKM/TK06/02/2/F00165.

REFERENCES

[1] K. Yi, J. Yoon and D. Kim, "Model-based Estimation of Vehicle Roll State for Detection of Impending Vehicle Rollover." *Proceeding of the 2007 American Control Conference,* IEEE, pp. 1624-1629, 2007.

[2] M.A. Abdullah, M.A. Salim, M.Z. Mohammad Nasir, M.N. Sudin, and F.R. Ramli, "Dynamics performances of Malaysian passenger vehicle," *ARPN Journal of Engineering and Applied Sciences*, ISSN 1819-6608, vol. 10, no. 17, pp. 7759-7763, 2015.

[3] H. Zhang, N. Zhang, F. Min, S. Rakheja, C. Su and E. Wang, "Coupling Mechanism and Decoupled Suspension Control Model of a Halff Car." *Mathematical Problems in Engineering,* vol. 2016, ID 1932107, 2016.

[4] M.A. Abdullah, J. F. Jamil, N. Ismail, M.Z. Mohammad Nasir, and M. Z. Hassan, "Formula varsity race car - Roll dynamic analysis." *Proceedings of Mechanical Engineering Research Day 2015: MERD'15*, pp. 23-24, 2015.

[5] M.A. Abdullah, J.F. Jamil and A.E. Mohan, *Vehicle Dynamics Modeling & Simulation*, Malacca: Centre for Advanced Research on Energy (CARe), Faculty of Mechanical Engineering, Universiti Teknikal Malaysia Melaka; ISBN: 978-967-0257-78-5; 2016.

Proceedings of Innovative Research and Industrial Dialogue'16, pp. 137-138 (May 2017)

The effect of rotary ultrasonic assisted machining on the thrust force generation of cutting D2 tool steel materials

R. Azlan[1,2,*], R. Izamshah[1], M. Hadzley[1], M.S. Kasim[1], M. Arfauz[1], M. Akmal[1]

[1)] Faculty of Manufacturing Engineering, Universiti Teknikal Malaysia Melaka, Hang Tuah Jaya, 76100 Durian Tunggal, Melaka, Malaysia.
[2)] Department of Mechanical Engineering, Politeknik Melaka, Balai Panjang, Plaza Pandan Malim, 75250 Melaka, Malaysia.

[*]Corresponding e-mail: azlan_ramli@yahoo.com

Keywords: Rotary Ultrasonic Assisted Machining (RUAM), AISI D2 hardened tool steel, thrust force, mould and die.

ABSTRACT – This paper demonstrates the effectiveness of rotary ultrasonic assisted milling (RUAM) technique in improving the machining performance on machining AISI D2 tool steel material for mould and die industry. The high strength of this material (>50 HRc) contributes to its poor machinability ratings. Some of the common problems in dealing with this material are roughed machined surface, high machining force, high cutting temperature and rapid tool wear. Experimental investigation to compare between RUAM and conventional machining for different set of parameters namely cutting speed, feed rate and machining depth on the magnitude of cutting force was conducted to confirm the effectiveness of the RUAM process. The design of experiment (DOE) technique use 2 level factorial design with 3 factors. The experimental results yielded the improvement of thrust force magnitude with up to 86% reduction when applying rotary ultrasonic assisted machining compared to conventional machining with the same cutting condition.

1. INTRODUCTION

The great challenges in the machining of tool steel materials in mould and die industry are to get an excellent mirror surface finish of machined surface and reduce a cutting force during machining of tool steel materials.

The effectiveness of machining performance such a surface roughness and cutting force is depending on milling machining parameters (cutting speed, feed rate and depth of cut) [1]. Currently, manufacturing sectors must produce high accuracy finished products and good surface quality [2]. Some problem faced in conventional machining of hardened tool steel material are rough machined surface, rapid tool wear, high machining force and high machining temperature. According to a study [3], ultrasonic assisted vibration cutting effectively reduces the cutting deformation and cutting force.

When mirror surface is required using conventional machining, the contact point between the tool and work piece will cause the excessive cutting force, and lead the high machining force with the rapid tool wear [4]. To solve this problem, rotary ultrasonic machining is needed to replace a conventional machining with an aim to improve a machining force.

The process of ultrasonic machining begins with a conversion of low frequency electrical energy to a high frequency electrical signal and its fed to transducer. While, the transducer converts high frequency electrical energy into mechanical vibration device and transmits it to the horn and later to cutting tools [6]. The horn and cutting tool vibrates along its longitudinal axis with high frequency of more than 20 kHz [5].

The principle of ultrasonic machining (USM) is different from rotary ultrasonic machining (RUM). The rotary ultrasonic machining (RUM) is a hybrid process combining ultrasonic machining (USM) with material removal mechanism and the tool is attached at the end face of the ultrasonic vibration spindle which will cause the tool to vibrate ultrasonically [7].

In conventional cutting machining process, the cutting force during machining increases at a quite higher rate especially the thrust force [3]. This paper aims to evaluate the thrust force between conventional machining and ultrasonic machining for different machining parameters (cutting speed, feed rate and depth of cut) on machining hardened D2 tool steel materials.

2. METHODOLOGY

All experiments were conducted using 3 axis CNC milling, model HAAS VF-1. The workpiece material used in this experiment was rectangular block of hardened D2 tool steel with 125 mm X 100 mm X 19 mm dimension and 51 HRC hardness. Ultrasonic tool holder assisted milling (BT40 ultrasonic tool holder) was attached to the CNC machining spindle to undergo slot milling test with different parameter values and experiments which was conducted by comparing conventional machining (without ultrasonic vibration) and ultrasonic assisted machining (with ultrasonic vibration). The experimental arrangement is shown in Figure 1. The experiment of slot milling was carried out using 2 flutes of carbide end mill with 6 mm diameter. The slot milling test was performed using ultrasonic frequency of 23.83 kHz and measured by digital multimeter. The ultrasonic vibration amplitude of 2 μm was used and dry cutting machining condition was applied. The design of experiments (DOE) using 2 level factorial design analysis with 3 machining parameters and 16 run was employed in these experiments. The cutting variables for slot milling test are shown in Table 1. The cutting force of the slot milling was measured by

Kistler 3 component Dynamometer Type 9257BA.

Table 1 Two level cutting applied in an experiment

Level	*Vc*, m/min	*f*, mm/min	a_p, µm
+1 (high)	0.6	5	10
-1 (low)	3	100	12

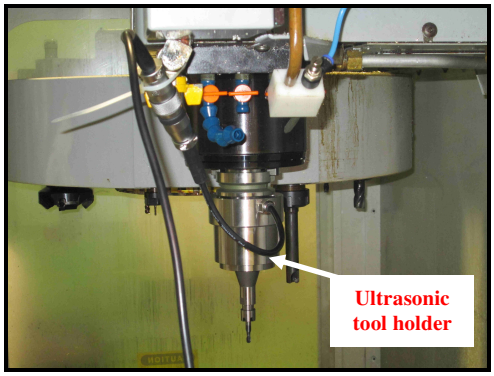

Figure 1 The experimental setup

3. RESULTS AND DISCUSSION

The results of thrust force (z-axis) is highlighted because the thrust force is the highest component force among the three force components. The results of thrust force are shown in Table 2 and graphically represented in Figure 2.

Table 2 Results of thrust force

Run	Vc (m/min)	f (mm/min)	Ap (µm)	Thrust Force, Fz (N)		
				Conventional (N)	Ultrasonic (N)	Reduction (%)
1	0.6	100	10	40.28	19.23	52.26
2	0.6	100	12	58.89	25.63	56.48
3	3.0	5	12	25.33	3.66	85.55
4	3.0	100	10	29.60	28.08	5.14
5	3.0	100	12	20.75	19.23	7.33
6	0.6	5	10	14.75	13.72	6.98
7	3.0	5	10	17.14	16.96	1.05
8	0.6	5	12	22.14	13.73	37.99

The magnitude of thrust force in conventional machining was quite higher compared to rotary ultrasonic assisted milling. The maximum value of thrust force for conventional machining at z-axis direction (Fz) was at Run 2 (Vc = 0.6 m/min, f = 100 mm/min, Ap (axial depth of cut) = 12 µm) about 58.89 N. The maximum value of thrust force for rotary ultrasonic assisted machining at z-axis direction (Fz) was at Run 4 (Vc = 3 m/min, f = 100 mm/min, Ap (axial depth of cut) = 10 µm was about 28.08 N. The experimental results yielded the improvement of thrust force magnitude with up to 86 % reduction when applying rotary ultrasonic assisted machining compared to conventional machining with the same cutting same cutting condition.

4. CONCLUSIONS

In conclusion, this study shows that feed rate is the main parameter that affects the magnitude of thrust force value. The thrust force increases when the feed rate increases. Hence, rotary ultrasonic assisted machining successfully improves the thrust force (Fz) with more reduction in magnitude of thrust force when machining hardened steel materials.

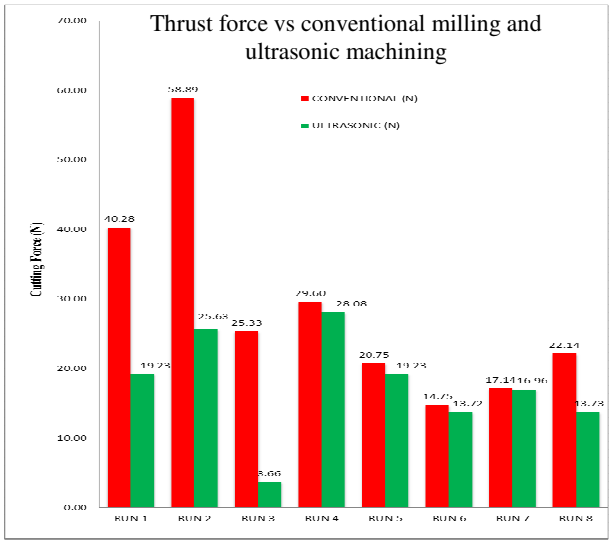

Figure 2 Comparison plots of thrust force

REFERENCES

[1] R. Izamshah, J.P.T. Mo, S. Ding, M. Arfauz, "Effect of Parameter Condition on Surface Roughness for Machining AISI D2 Hardened Steel," *J. Adv. Manuf. Technol.*, vol. 8, no. November, pp. 47–56, 2010.

[2] R.Azlan, R.Izamshah, M.Hadzley, M.S. Kasim, M. Arfauz, "Experimental investigation of surface roughness using ultrasonic assisted machining of hardened steel," *Proc. Mech. Eng. Res. Day 2016*, vol. 1, no. March 2016, pp. 212–213, 2016.

[3] M. Zhou, Y. T. Eow, B. K. A. Ngoi, and E. N. Lim, "Vibration-Assisted Precision Machining of Steel with PCD Tools," *Mater. Manuf. Process.*, vol. 18, no. 5, pp. 825–834, 2003.

[4] R. Ibrahim, N. H. Rafai, E. A. Rahim, K. Cheng and H. Ding, "A Performance of 2 Dimensional Ultrasonic Vibration Assisted Milling in Cutting Force Reduction, on Aluminium Al6061," *ARPN J Eng. Appl. Sci.* vol. 11, pp 11124-11128, 2015.

[5] R. Singh and J. S. Khamba, "Ultrasonic machining of titanium and its alloys: A review," *J. Mater. Process. Technol.*, vol.173, no.2, pp. 125–135, 2006.

[6] M. Nad, "Ultrasonic horn design for ultrasonic machining technologies," *Appl. Comput. Mech.*, vol. 4, no. 1, pp. 79–88, 2010.

[7] Y. Jiao, W. J. Liu, Z. J. Pei, X. J. Xin, and C. Treadwell, "Study on Edge Chipping in Rotary Ultrasonic Machining of Ceramics: An Integration of Designed Experiments and Finite Element Method Analysis," *J. Manuf. Sci. Eng.*, vol. 127, no. 4, p. 752, 2005.

Effect of repetitive rework on microhardness of dissimilar austenitic Stainless Steel pipes using GMAW orbital welding

S.Laily*, N.I.S.Hussein, M.N.Ayof, T.H.Kean

Faculty of Manufacturing Engineering, Universiti Teknikal Malaysia Melaka,
Hang Tuah Jaya, 76100 Durian Tunggal, Melaka, Malaysia

*Corresponding e-mail: surayalaily@gmail.com

Keywords: Stainless Steel Pipe; Orbital Welding; Gas Metal Arc Welding; Repetitive Rework

ABSTRACT – Fabrication of part by using dissimilar material are lighter and more economical. Furthermore, repair welding on dissimilar material is more challenging than similar material and they give different residual stress properties as compared to joining similar material. AISI 304 and AISI 316L are austenitic stainless steels with slight difference in composition. In this article, the effect of repair welding on microhardness of dissimilar stainless steel pipes has been studied.

1. INTRODUCTION

Orbital welding is the most applicable joining process in industry whenever high quality of welding results is desired. Orbital welding is defined based on the circular movement of welding tool or welding torch around the workpiece to be welded. Since pharmaceutical equipment always subjected to high temperature and pressure, they are more susceptible to premature failure after a certain service period and it becomes more critical when there is involvement of dissimilar metal weld joints. This is because dissimilar metal weld joints have higher tendency encountered to material degradation such as thermal aging [1].

Austenitic stainless steels have good performance in corrosive working environment. This type of stainless steel is applicable in either conducive or elevated temperature service environment. Besides that, they have also good mechanical properties particularly ductility and toughness, so that it shows remarkable elongation during tensile testing. Indeed, practice of DMW with formation of dissimilar metal joint allows the transition in mechanical properties or in service conditions as required in certain applications [2].

Repairing activity with welding process is often desired in industry to prolong the service lives or enhance performance of the components. Defects on weldment such as porosity, lack of penetration, slag inclusion and incomplete fusion may develop in pipeline fabrication [3]. On the basis of the comprehensive literature review, the study of repair welding on steel material had rarely been reported. The main objective of this paper is to study the effect of welding repairing activities on microhardness of dissimilar stainless steel pipes.

2. EXPERIMENTAL

Turning process using a lathe machine was carried out to get the pipes in original condition as showed in Figure 2. Material with first time repaired marked as RW1 and followed with RW2 for two times repair, RW3 for three times repair and RW4 for four times repair. Throughout the whole process of repair welding, machine was set up with constant parameter where current with 133A, voltage with 21V and speed with 2700mm/min.

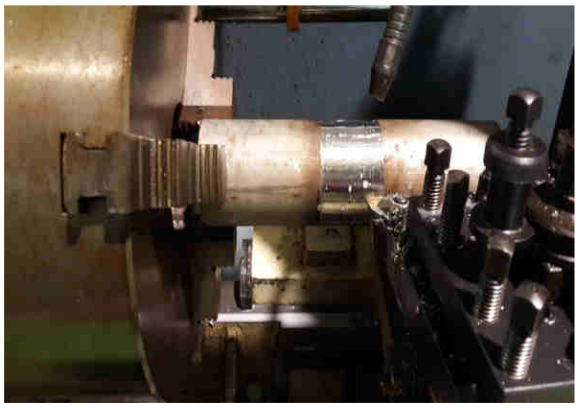

Figure 1 Welded pipe after lathe turning

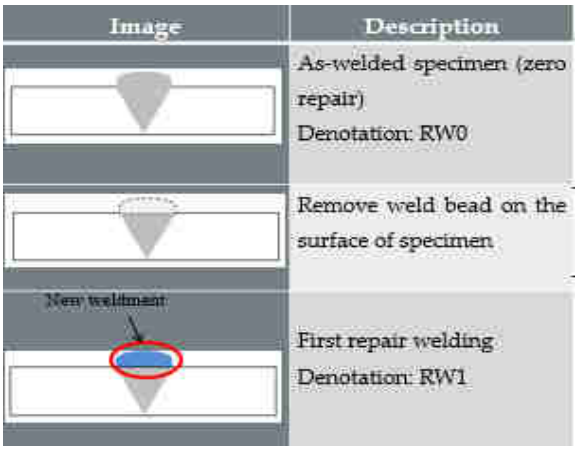

Figure 2 Repair welding procedure

Figure 2 shows repair welding procedure using GMAW orbital welding. As first repair welding, weld bead on first specimen was removed by turning process. The process is continued for every stage of repair welding with setting of parameter of arc current 133A, arc voltage 21V and welding speed 25mm/min.

3. RESULTS AND DISCUSSION

Table 1 shows microhardness value for AISI 304 and AISI 316L. Differences in microhardness values were due to carbon content where AISI 304 has higher than AISI 316L [4,5]. Microhardness testing was performed by using HM-221 Vickers microhardness tester with 500gf load was applied.

Table 1 Microhardness of AISI 304 and AISI 316L

Base Metals	Microhardness (VHN)
AISI 304	182
AISI 316L	176

Table 2 shows the summary of the average of microhardness values for all of the specimens. Apparently, microhardness for RW1 is comparatively lower than RW0 as shown in Figure 3. This is due to presence of lathy delta ferrite that contributes to high microhardness. Differences in microhardness values in fusion zone and base metal is due to repeated thermal cycle applied where overheat treatment can cause lowest microhardness. Besides, increasing number of repair welding has increased the microhardness.

Table 2 Summary of microhardness average value ($HV_{0.5}$)

Weld repair	Microhardness Values		
	HAZ at vicinity of AISI 304	Weldment	HAZ at vicinity of AISI 316L
RW0	168.6	148.9	158.0
RW1	145.6	144.7	163.9
RW2	150.1	148.2	165.7
RW3	157.1	153.2	154.6
RW4	161.0	158.8	154.3

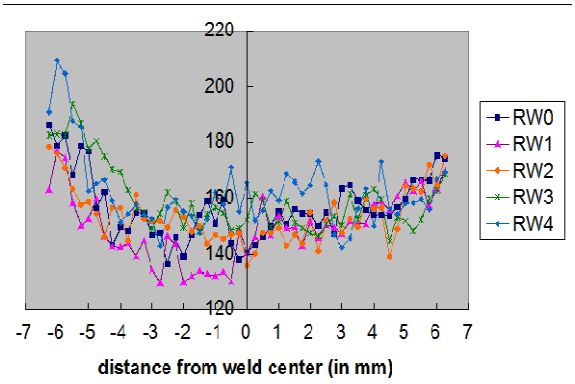

Figure 3 Combination of the line graphs of microhardness measurement profiles

4. CONCLUSION

From the result obtained, AISI 304 has higher microhardness and better strength than AISI 316L. This is because of carbon content in AISI 304 is higher 0.05 wt% than AISI 316L. There was no apparent grain growth at both sides of HAZ, but grain refinement was contributed to its higher microhardness. Microhardness is increased with increase of repair welding.

ACKNOWLEDGEMENT

Authors are grateful to the Faculty of Manufacturing Engineering, Universiti Teknikal Malaysia Melaka for the facilities support. This research is funded through FRGS Grant numbered FRGS/1/2015/TK03/FKP/02/F00280.

REFERENCES

[1] A. Aloraier, A. Al-Mazrouee, J.W.H. Price, T. Shehata, "Weld repair practices without post weld heat treatment for ferritic alloys and their consequences on residual stresses: A review", *Int.Journal of Pressure Vessels and Piping*, no. 87, pp. 127-133, 2010.

[2] H. Eisazadeh, J. Bunn, H.E. Coules, A. Achuthan, J. Goldak, and D.K. Aidun, "A Residual Stress Study in Similar and Dissimilar Welds," Welding Research Journal, vol. 95, pp. 111-119, 2016.

[3] P. Varghese, M.S. Prasad, F. Joseph, M.J. Varkey, K. Anthony, and A. Sreekanth, "The effect of repeated repair welding on the corrosion behavior of austenitic stainless steel and mild steel dissimilar weldment", *Proceeding of International Conference on Advanced in Materials, Manufacturing and Applications*, 2015, pp. 864-869.

[4] S. Debnath, M. Mukherjee, and T.K. Pal, "Study on microstructure and mechanical properties of thick low-alloy quench and tempered steel welded joint", *Material Performance and Characterization,* vol 3(1), pp. 23-48, 2004.

[5] C.C. Hsieh, D.Y. Lin, M.C. Chen, and W. Wu, "Microstructure, recrystallization, and mechanical property evolutions in the heat-affected and fusion zones of dissimilar stainless steels", *Materials Transactions,* vol. 48(11), pp. 2898-2902, 2007.